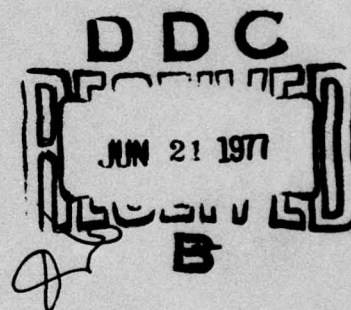AFGL-TR-77-0025
ENVIRONMENTAL RESEARCH PAPERS, NO. 591

Vibrational Excitation of Carbon Dioxide and Carbon Monoxide by High Velocity Collision With Molecular Oxygen

A. RAHBEE
JAMES J. GIBSON
CHARLES P. DOLAN

26 January 1977

DDC

JUN 21 1977

B

OPTICAL PHYSICS DIVISION   PROJECT 2303

AIR FORCE GEOPHYSICS LABORATORY
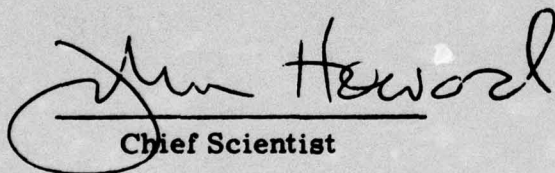HANSCOM AFB, MASSACHUSETTS 01731

AIR FORCE SYSTEMS COMMAND, USAF

ADA040779

AD No.
DDC FILE COPY

This report has been reviewed by the ESD Information Office (OI) and is releasable to the National Technical Information Service (NTIS).

This technical report has been reviewed and is approved for publication.

FOR THE COMMANDER

Chief Scientist

Unclassified

REPORT DOCUMENTATION PAGE	READ INSTRUCTIONS BEFORE COMPLETING FORM

1. REPORT NUMBER	2. GOVT ACCESSION NO.	3. RECIPIENT'S CATALOG NUMBER
AFGL-TR-77-0025	AFGL-ERP-591	

4. TITLE (and Subtitle)	5. TYPE OF REPORT & PERIOD COVERED
VIBRATIONAL EXCITATION OF CARBON DIOXIDE AND CARBON MONOXIDE BY HIGH VELOCITY COLLISION WITH MOLECULAR OXYGEN	Scientific. Interim.
	6. PERFORMING ORG. REPORT NUMBER
	ERP No. 591

7. AUTHOR(s)	8. CONTRACT OR GRANT NUMBER(s)
A. Rahbee James J. Gibson Charles P. Dolan	

9. PERFORMING ORGANIZATION NAME AND ADDRESS	10. PROGRAM ELEMENT, PROJECT, TASK AREA & WORK UNIT NUMBERS
Air Force Geophysics Laboratory (OPR) Hanscom AFB, Massachusetts 01731	61102F 2303G201

11. CONTROLLING OFFICE NAME AND ADDRESS	12. REPORT DATE
Air Force Geophysics Laboratory (OPR) Hanscom AFB, Massachusetts 01731	26 January 1977
	13. NUMBER OF PAGES
	27

14. MONITORING AGENCY NAME & ADDRESS(if different from Controlling Office)	15. SECURITY CLASS. (of this report)
Environmental research papers	Unclassified
	15a. DECLASSIFICATION/DOWNGRADING SCHEDULE

16. DISTRIBUTION STATEMENT (of this Report)

Approved for public release; distribution unlimited. 28p.

17. DISTRIBUTION STATEMENT (of the abstract entered in Block 20, if different from Report)

18. SUPPLEMENTARY NOTES

19. KEY WORDS (Continue on reverse side if necessary and identify by block number)
Molecular beams
Short wave infrared
Reaction cross section
Vibrational excitation

20. ABSTRACT (Continue on reverse side if necessary and identify by block number)
A hyperthermal molecular beam apparatus, utilizing a heated seeded supersonic nozzle capable of producing fast intense beams of atmospheric species, has been employed to study vibrational excitation of plume species carbon dioxide and carbon monoxide. The apparatus is provided with a novel neutral beam detector for measurement of beam intensity and velocity distribution. The excitation mechanism is studied through monitoring of the infrared emission from the plume species by the use of lead sulfide, lead selenide, and indium antimonide. Lack of measurable signals is analyzed in terms of signal

DD FORM 1 JAN 73 1473 EDITION OF 1 NOV 65 IS OBSOLETE

20.   (Cont)

to noise ratios and it is shown that excitation cross sections generally have an upper limit of 10^{-19} cm^2 showing that transfer of translational energy into internal energy does not take place efficiently.

10 to the 19th power per square centimeter

Contents

Illustrations

Vibrational Excitation of Carbon Dioxide and Carbon Monoxide By High Velocity Collision With Molecular Oxygen

1. INTRODUCTION

The molecular beam method for the study of atomic and molecular collision phenomena has been utilized for the last several decades in numerous laboratories. Despite the impressive amount of data obtained over this span of time, the use of molecular beams has been generally restricted to two energy regions. These are the thermal region covering the collision energy of a fraction of an electron volt and the high energy region which generally covers the energies above 100 eV. In addition, the beam species that could be utilized in a molecular beam were limited to those which could be easily detected. These were generally alkali metals and their compounds, which can be detected with efficiencies approaching one hundred percent. Investigation of the collision of species other than these and involving energies of a few electron volts has only met partial success for lack of techniques for producing intense beams with adequate energies and the difficulty in the detection of beam species. There are numerous collision phenomena that require very high intensity molecular beams with laboratory energies of 1 to 5 eV (corresponding to collision velocity of 1 to 6 km/sec). Among these are many chemical reactions and numerous inelastic collisions in which translational energy is converted into internal energy of one or both colliding partners. As a consequence the vibrational or rotational state of the molecules is changed and the collision eventually leads into the emission of the characteristic infrared radiation. Study of such

infrared producing collisions is currently of great interest in the interaction of rocket plume species and atmospheric constituents. This interaction takes place with relative collision velocity of 1 to 6 km/sec. Laboratory study of these vibrational and rotational excitation collisions requires beams of atmospheric particles such as O_2, N_2, O with velocities corresponding to rocket velocities, and efficient methods for their detection.

The present report is a description of an experimental program to study the vibrational excitation of plume species under bombardment by fast beams of atmospheric particles. In the sections that follow, the vacuum system, molecular beam generator, and detector are dealt with in some detail. The last section is a discussion of the results in terms of upper limits on excitation cross sections and analysis of signal to noise ratios, and includes some suggestions for future work for definitive determination of excitation cross sections.

2. GENERAL DESCRIPTION OF THE VACUUM SYSTEM

The experimental apparatus for the study of high velocity interaction of plume/atmosphere species is shown in Figure 1. The apparatus consists of three differentially pumped chambers to maintain proper pressures consistent with experimental requirements in each chamber. The first chamber houses the hyperthermal molecular beam source and its associated chopping disks and beam defining elements whose functions will be dealt with in the following sections of this report. The second chamber is a spherical gold-plated glass sphere in which target plume gases are introduced and is called the collision chamber. After traversing this chamber, the fast molecular beam emerges into a third chamber, called detection chamber, where its intensity and velocity can be measured. These three chambers are shown schematically in Figure 2.

The beam generation chamber is a stainless steel cylindrical chamber 3 ft in diameter which is pumped on by an NRC HS-32 fractionating oil diffusion pump with a nominal speed of 32,000 l/sec. This pumping speed is reduced to one-half the nominal value by a liquid-nitrogen cooled baffle. The fore pump is a Kinney KDH 150 mechanical pump with a speed of 70 l/sec. The vacuum system foreline is valved by a solenoid actuated slide valve. Ultimate pressure in this chamber is 5×10^{-8} torr without gas flow and operating pressure with beam gas on is in the 10^{-4} torr range. The high pumping speed is required for removal of large quantities of source gas while maintaining acceptable background pressures.

The collision chamber, which is a 16-cm diameter gold plated sphere and communicates with the source chamber through a collimating orifice for beam entrance, is pumped on by a NRC HS-6 oil diffusion pump with maximum pumping speed of 1500 l/sec, backed by a Welsh Duo-Seal 15 ft^3/min mechanical pump.
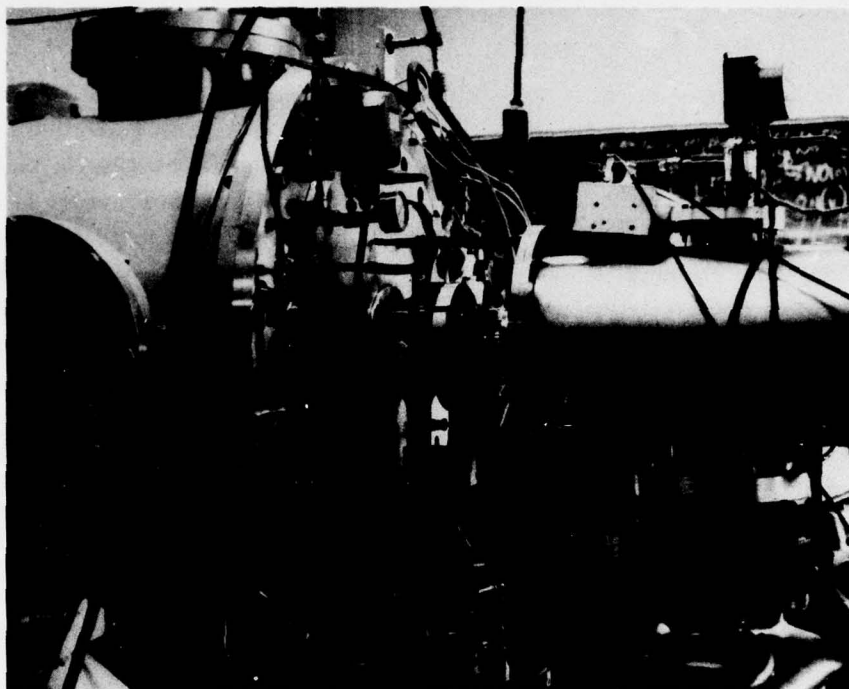
6

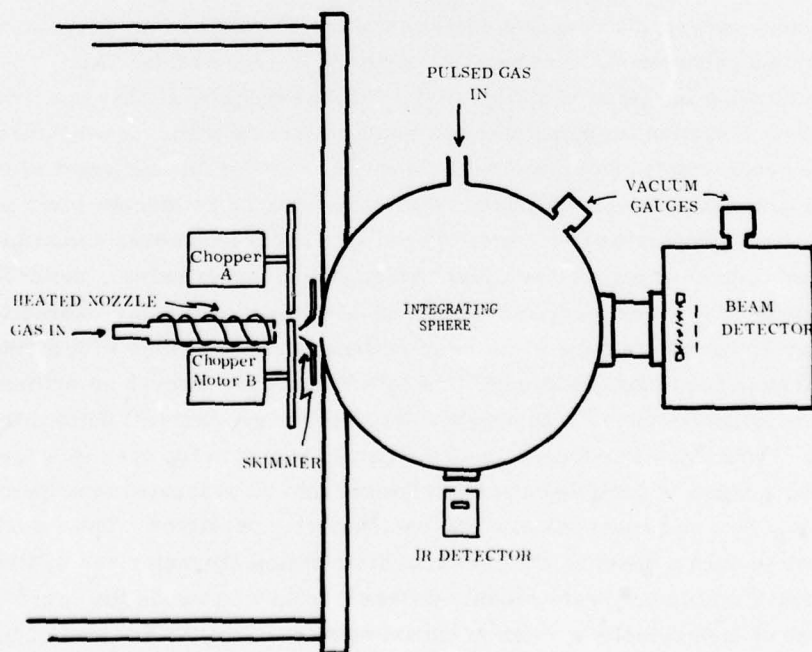Figure 1. High Velocity Molecular Beam Apparatus

Figure 2. Schematic of the Experimental Apparatus Showing the Beam
Generator, Collision, and Detection Chambers

The diffusion pump is also provided with a liquid-nitrogen cooled baffle which in effect reduces the pumping speed by a factor of two. Ultimate pressure in the collision chamber is 5×10^{-8} torr without the beam and rises to 10^{-6} torr with beam on. The chamber is also provided with an aperture to allow the molecular beam to exit into the detection chamber.

The detection chamber, which houses a specially designed molecular beam ionizer detector, is a 1-ft diameter cylindrical chamber, constructed from stainless steel. It is pumped on by an NRC VHS-6 oil diffusion pump with maximum speed of 2500 l/sec unbaffled and 1500 l/sec with liquid nitrogen cooled baffle. It is backed by a Welsh Duo-Seal 15 ft^3/min mechanical pump. Ultimate pressure in this chamber is 10^{-7} torr.

All pressures are measured by NRC 507 ionization gauges except the pressure in the molecular beam source itself. This pressure is measured by a pre-calibrated Baratron gauge capable of measuring pressures with 5 percent accuracy.

3. MOLECULAR BEAM GENERATION

3.1 Background

Molecular beams, as research tools in the investigation of atomic and molecular collision phenomena, have been in existence for several decades. The main advantage of using beams of particles is the ability they provide the experimenter to study the interaction (in principle) of a single molecule with another molecule. Molecular beam experiments provide the means for direct measurement of some molecular properties which, through statistical averaging technique, yield macroscopic (or bulk) properties of matter. These statistical techniques sometimes obscure the molecular properties under investigation, nevertheless, molecular beams provide the closest approach to individual atomic/molecular interactions.

Molecular beams (that is, streams of collision-free particles with defined velocities) have been classically produced by effusive flow through an orifice in a pressurized chamber (oven) with appropriate slits for geometrical definition of the beam. When the mean-free-path of the particles inside the oven is larger than the orifice, a beam of particles can be delivered into an evacuated test chamber and the beam flux and beam velocity can be accurately predicted. The velocity distribution in such a beam is a Maxwellian distribution characterized by the source temperature T and is only very slightly different from that inside the "oven". For the purpose of high velocity excitation experiments that are the purpose of the present experiment, classical oven sources have three major drawbacks. These are the hopelessly small beam intensities, the large velocity distribution, and the very low energies attainable. Intensities are typically 10^{11} to 10^{12} particles/cm^2 sec,

8

the velocity range extends from zero on upward and beam energies are only a fraction of an electron volt. Narrow distribution can be attained by velocity selectors that allow a narrow band of velocities to be transmitted into the collision chamber but this further diminishes the beam intensity by orders of magnitude. Higher energies also can be achieved by heating the "oven", thus moving the speed distribution centroid to higher values, but achieving energies of the order of a few electron volts requires temperatures of tens of thousands of degrees, which is prohibitive.

The higher end of the energy spectrum (covering 100 eV beams and higher) has also been reached through the entirely different method of charge exchange, in which an ion beam of the desired species is extracted from an ion source, accelerated, and neutralized through electron exchange with a neutral gas. Contrary to "oven" beams, charge exchange beams are too energetic for our purpose. Lowering the ion energy by retardation potentials causes severe drops in beam intensity due to space charge effects. In addition, the original ion beam (which is usually extracted from a discharge source or an electron bombardment source) contains unknown excited species or metastable particles, and the final internal state of the beam particles is the subject of considerable doubt and uncertainty.

The limitations of the classical "oven" sources, namely low beam intensity and wide velocity distribution, were alleviated by the suggestion of Kantrowitz and Gray[1] to replace the effusive flow of a conventional oven beam by the flow from a supersonic jet. The idea was to convert the internal energy of the gas in the nozzle into directed mass motion thus increasing the intensity and velocity of the emerging beam and due to severe temperature drop during the isentropic expansion from the nozzle, to obtain much narrower velocity distribution.

This suggestion by Kantrowitz and Gray was first tested by Kistiakowsky and Slichter[2] whose efforts met with only partial success due to lack of pumping speed in their vacuum system. Later the usefulness of supersonic jets as beam sources was convincingly demonstrated by Becker and Bier,[3] whose pioneering work initiated an intensive and systematic series of theoretical and experimental investigations of several aspects of this new molecular beam source.[4]

Figure 3 shows a schematic representation of a nozzle beam system and its elliptical flow field. The element called skimmer allows the central portion of the flow to enter into the test chamber and replaces the orifice in a classical oven source. The pressure in the plenum chamber of the nozzle is much higher than the corresponding pressure in an oven beam such that the mean free path in the nozzle

1. Kantrowitz, A. and Gray, J. (1951) Rev. Sci. Instr., 22:238.
2. Kistiakowsky, G. B. and Slichter, W. P. (1951) Rev. Sci. Instr., 22:333.
3. Becker, E. W. and Bier, K. (1954) Z. Naturforsch, 9a:975.
4. Anderson, J.B., Andres, R.P., and Fenn, J.B. (1966) Molecular Beams, J. Ross, Ed., Interscience, New York

is much smaller than the sonic orifice. The flow from this orifice starts in the continuum regime and after going through a transition regime finally becomes free molecular. In some of the early work on nozzle beams converging-diverging nozzles were employed. Becker and Bier essentially obtained the same intensities when they cut off the diverging section of the nozzle. [3] The majority of nozzle beam sources in existence employ just a sonic orifice instead of diverging nozzles. Simple sonic orifices appear to be most useful because they avoid boundary layer problems of the diverging nozzles and are easier to manufacture. The general flow characteristics of the flow from such orifices are reasonably predictable. Quantities such as local temperature density and pressure on the jet axis can all be expressed in terms of Mach number. The Mach number itself is also expressible as a function of axial distance from the nozzle orifice. [5] Ashkenas and Sherman have developed analytical expressions which describe some flow field properties such as density and temperature and radial Mach number distribution. [6] The results, without going into calculational details, can be summarized as follows.

SKIMMER

NOZZLE

TEST CHAMBER

PUMP   PUMP   PUMP
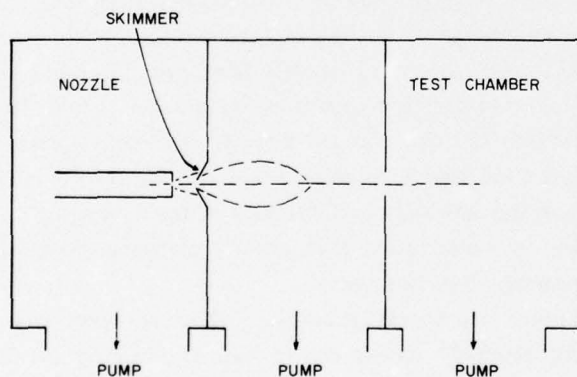
Figure 3. Schematic Representation of a Nozzle Beam System Showing the Relative Intensity Distribution in the Flow Field

For the region of the flow, before the terminal Mach number is reached, the distribution of density in the axial direction can be calculated by assuming the flow field originates from a point source near the nozzle exit plane. The density decreases as $1/X^2$, where X is axial distance to the exit plane. When density decreases to a value determined by nozzle size and plenum chamber pressure, a transition occurs from continuum flow to free molecular. Beyond this region density continues its inverse square with distance but the temperature remains constant and Mach number reaches its terminal value. At a distance slightly beyond

5. Sherman, F.S. (1963) Rarified Gas Dynamics, J.A. Laurman, Ed., Vol. II, Academic Press, New York.

6. Ashkenas, H. and Sherman, F.W. (1966) Rarified Gas Dynamics, J.H. deLeeuw Ed., Academic Press, New York.

the transition region, the jet density becomes low enough and background gases begin to scatter the jet molecules causing a drop in intensity. Thus the location of the beam defining element called skimmer becomes important.[4]

The reason for large pumping speeds becomes clear when we consider the large axial velocity the jet acquires in an isentropic expansion. Mass flow through the orifice goes directly with this flow velocity necessitating pumping speeds an order of magnitude larger than that needed in classical oven sources. In addition to this axial velocity, the velocity distribution is considerably narrowed due to the temperature drop during the expansion process.

For a beam of helium the maximum velocity in a nozzle beam is $\simeq$ 1.7 km/sec for room temperature nozzle. This velocity is 0.6 km/sec for O_2 nozzle beam and 0.65 for an N_2 beam. These velocities are obviously too small for the purposes of the vibrational excitation experiments which require velocities in the range of 2 to 5 km/sec. Increasing the nozzle temperature by a factor n enhances the beam velocity of $\sqrt{n}$. Thus for a helium beam from a nozzle at 1500 K the maximum beam velocity will be slightly above 4 km/sec. For an H_2 beam the final velocity of 6 to 7 km/sec can be achieved. But for pure beams O_2 and N_2 (because of their heavy masses) this final velocity can be in the 1 to 2 km/sec range.

To attain higher velocities and energies, it appears that Anderson, Andres, and Fenn[4] were first to propose a novel approach with a supersonic nozzle. They proposed the use of a heated nozzle source and a gas mixture comprised of a light gas diluted by a small percentage of the heavy species O_2, N_2, and so forth. When such a binary mixture is expanded from a nozzle, there are sufficient collisions during the expansion of the jet to maintain equilibrium between the two species and at the entrance of the skimmer both gaseous species will have the same velocity. The mean jet velocity will be equal to that of the light component as long as dilution is small and on the order of a few percent. The actual values of velocity and temperature will correspond to those of a pure gas with molecular weight and specific heat ratio of weighted averages of the mixture species. If, for example, one percent N_2 is used in helium, nitrogen molecules will have a velocity of 1.6 km/sec from a room temperature nozzle. If the nozzle is heated to 2000 K, this velocity will be approximately 5 km/sec for nitrogen. If lighter carrier gas (such as H_2) is used this velocity will be even higher. This idea for production of high energy heavy particles was pursued in several laboratories[7,8,9] and is the one adopted by us for the collisional excitation experiments.

7. Klingelhofer, R. and Lohse, P. (1964) Phys. Fluids, 7:379.

8. Albright, R. G., Peeters, J., Bourguignon, M., LeRoy, R. L., and Deckers, J. M. (1966) Rarefied Gas Dynamics, J. H. deLeeuw, Ed., Academic Press, New York.

9. French, J. B. and O'Keefe, D. R. (1966) Rarefied Gas Dynamics, J. H. deLeeuw, Ed., Academic Press, New York.

At first glance, it may seem that a small concentration of heavy species might result in low beam intensities, but due to the nature of the collisions in the expanding jet the percentage of the heavy component in the final beam will be much higher than in the source. This so-called preferential focussing of the heavy species is due to the fact that they undergo smaller angular deflection during a collision with light particles. The extent of this focussing is roughly determined by the molecular weight ratio of the gases. Thus a 3 percent mixture of argon and 97 percent helium in the source would result in 30 percent argon in the final beam. With nozzle temperatures of 1500 K and higher the beam velocities achieved are in the 4 to 5 km/sec region which is in the range of interest in the present experiment.

3.2 The Molecular Beam Source

The schematic of the heated supersonic nozzle molecular beam source constructed for the high velocity collisional excitation experiment is shown in Figure 2. The source assembly with its associated carriages for three-dimensional movements is shown in Figure 4. The nozzle itself is a high temperature ceramic tube with an outside diameter of 1 cm and inside diameter of 0.65 cm. The closed end has an orifice of diameter 0.18 mm which serves as the nozzle throat diameter. The other end of the tube, which is connected to the gas mixture supply, is also immersed in a water-cooled brass block for heat sinking. The nozzle tube is wrapped with 30 turns of 0.02-in. diameter tungsten wire which carries the heating current. The nozzle could be heated to 1200 K with prolonged operation and temperature could be raised to 1500 K with shorter operating times. Temperature is monitored by an optical pyrometer which determines the temperature to within ± 50 K. The entire nozzle assembly is mounted on a carriage capable of moving in three x-y-z directions for nozzle alignment purposes. These movements, which are motorized and operable from outside the vacuum system, are accomplished by three Superior Electric stepping motors modified for use in vacuum. In addition to this capability, another movable carriage on which two rotating chopping disks are attached, provides the beam modulation capability for lock-in amplification and phase sensitive detection. One of these chopping disks is an aluminum disk with 8 circular openings on a 4-cm radius circle and with 50 percent duty cycle. This chopper is used for beam intensity measurement. A second chopper, also made of aluminum and the same overall size as the first, has 6 equally spaced radial slots, instead of circular openings, each 0.25 mm wide. This chopper is rotated by a variable speed motor and is used for beam velocity measurements. The purpose of the narrow slots is to provide short open times. Beam segments passing through these slots continue travelling to the beam detector where their time of flight is registered. The t = 0 for this time of flight is provided by a photo pulse obtained from a miniature tungsten light bulb chopped by the same slotted disk. Either of

12

these two choppers could be moved into the molecular beam path and both intensity and velocity distribution could be measured within minutes of each other.
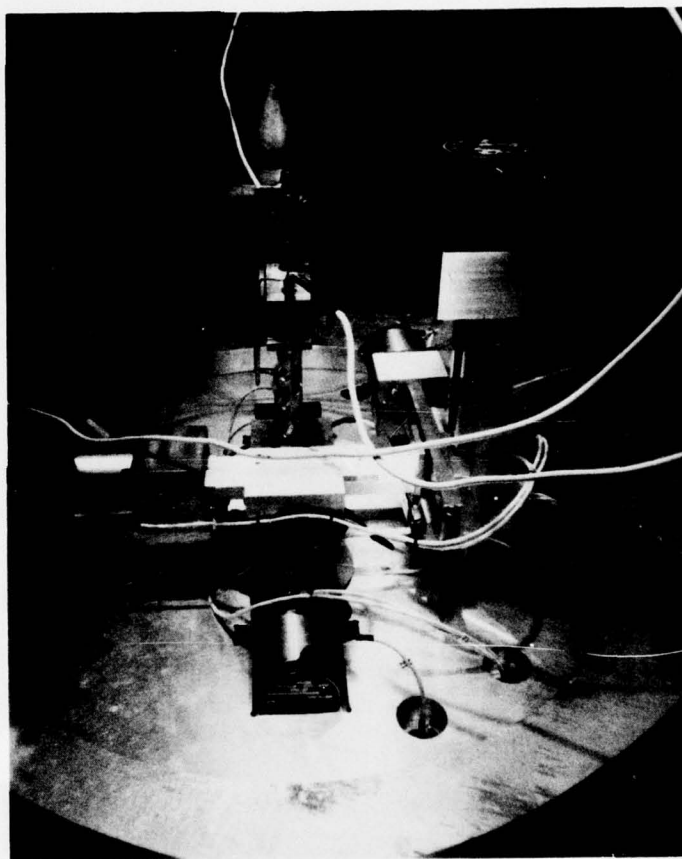
Figure 4.   Photograph of the Beam Generation Chamber
Showing the Nozzle and Its Associated Equipment

The second important beam defining element is the skimmer (see Figure 2). This is in the shape of a truncated cone with inside and outside half angles of 35 and 40 deg, respectively. Its opening is 0.06 cm and it is made of brass. The function of this element is to "skim off" the core of the expanded supersonic jet in the form of a molecular beam entry into the collision chamber. The beam collimator is presently an aperture in the spherical collision chamber, which also acts as the team entrance port, and its size is primarily determined geometrically to allow the entire skimmed beam to enter the collision chamber.

13

The nozzle skimmer distance is generally variable from 0.5 cm to 2 cm and the proper operating distance is dictated by the requirements of maximum intensity and narrow velocity distribution for each gaseous species employed. For the majority of species used this distance was generally from 1 to 1.5 cm

4. COLLISION CHAMBER

The collision chamber is a spherical chamber of 16-cm diameter made of glass, gold-coated on its inside surface for better photon collection efficiency. Target gases CO_2 or CO are introduced in this chamber at low pressures, usually below 1 mtorr, to prevent degradation of the incident fast molecular beam. Low target pressure is necessary from another point of view. Since the object of the experiment is to monitor infrared emission from vibrationally excited target molecules, further collisions of these species with residual gases must be prevented. The chamber is pumped on separately and is provided with ports for gas introduction and pressure monitoring. It is also provided with a CaF window for monitoring infrared emission.

The collision chamber, which in fact is an integrating sphere, has two important properties. Since the excited target molecules are produced along the incident beam path, the radiation output from the sphere into the IR detector must be independent of the source position. This is accomplished by "dimpling" the inside surface of the sphere to cause multiple reflection of the photons and make the radiation density uniform inside the chamber. This property of the sphere is confirmed by moving a miniature tungsten bulb inside the sphere and monitoring the radiation through several of the openings.

The second property of the sphere is improving the collection efficiency of the system. This property, which is usually characterized in terms of a "gain" factor, is the IR detector response with the gold-coated sphere compared with its response without the sphere. For the present integrating sphere, rather than measuring this gain factor, an efficiency factor, defined as the sphere output divided by known input into the sphere, is measured. This quantity is more or less close to 0.01 and takes into account all reflection and transmission losses in the optical system. The efficiency factor over a period of operation is degraded by deposition of pump oil vapors on the gold surface, reducing its reflectivity. For this reason the sphere is dismantled periodically and cleaned and freshly gold-coated.

For the purpose of phase-sensitive detection of the infrared emission from target molecules, a method was devised to modulate the target pressure gas in the chamber. Chopping the fast beam by mechanical choppers A and B (see Figure 2) would simultaneously modulate the radiation from the hot nozzle resulting in

huge background noise, orders of magnitude larger than the signals sought. The
solenoid operated gas valve for injecting gases into the collision chamber has been
described in detail elsewhere. [10] It has the capability of injecting gases at variable
frequencies over a wide pressure range, has a variable duty cycle, and provides a
reference signal for synchronous triggering of the lock-in amplification system.

As mentioned in the section on vacuum systems, the collision chamber pres-
sure is monitored through a Baratron, whose pressure sensing element is directly
exposed to the gas and which has very fast response time so that pressure pulses
can be followed very accurately. A sample of pressure pulses is shown in Figure 5
where the instantaneous value of the pressure against time is recorded. The
pressure at the peak could be set at will and the minimum is primarily determined
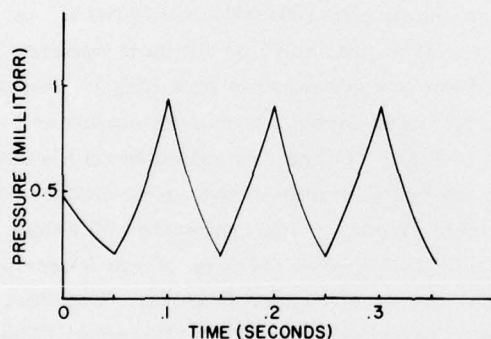by the residence time in the sphere and the modulation frequency.

Figure 5. Modulated Target Gas
Pressure

5. MOLECULAR BEAM DETECTION SYSTEM

5.1 Detector Design

The fundamental problem of molecular beam experiments is the difficulty of
quantitative measurements of the beam intensity. Historically, the majority of
beam experiments have been done with alkali metal beams because of the ease of
their detection by surface ionization detectors, based on the pioneering work of
Taylor. [11] For permanent gases with which the present experiment is involved,
the most suitable mode of detection is the "universal detector" also sometime re-
ferred to as electron bombardment detector. With this type of detector, which can
be used for any beam species, the neutral molecular beam is crossed with a suit-
ably arranged electron beam thus ionizing a portion of the neutral molecules. Ions

10. Dolan, C. P. (1971) Rev. Sci. Instr. 42:1228.
11. Taylor, J. B. (1930) Phys. Rev. 35:375.

produced in this way are then extracted and the ion current measured. The magnitude of this ion current is then related to the neutral beam intensity through suitable calibration methods. One such method is the use of a thermal oven beam whose intensity can be accurately calculated.[12]

Requirement for a molecular beam detector of this type is strongly dependent upon the type of experiment. For elastic scattering measurements where high angular resolution is necessary, very narrow entrance aperture and long ionization region in the beam direction are desired. The latter requirements are in conflict with accurate velocity distribution measurements. Since, in the present experiment, angular resolution is not very important but accurate velocity distribution is, a compromise has been achieved in which large ion currents can be obtained by admitting the entire beam into the detector while the length of the ionization region is made as short as possible.

The overall view of the detector incorporating these features is shown in Figure 6. Details of the ionization region are shown schematically in Figure 7. In this figure, which is the side view of the electron gun, the line filament appears as a point. Electrons emitted from this filament are accelerated by a long U-shaped repeller located behind the line filament, and pass through a channel cut in the anode block (cross-hatched region shown in Figure 7) and are collected on a second U-shaped plate symmetrically located on the opposite side of the anode block. The sheet of electrons is confined by a permanent magnet of field strength 300 gauss. The cathode assembly is entirely symmetric such that in the case of one filament burn-out, the detector can be operated with the second spare filament. The neutral molecular beam enters the ionization region perpendicular to the electrons. The resulting ions, after extraction, are collected on the collecting sensor. Because of the specially shaped anode block the equipotential surfaces shown as dashed lines tend to focus the resulting ion beam.

The entire ionization chamber is supported on the permanent magnet yoke and teflon insulators are used wherever necessary.

5.2 Beam Detector Operation

Quantitative measurement of excitation cross section from molecular beam experiments generally requires the knowledge of the beam flux entering the collision chamber and the beam velocity. The detector described in Section 5.1, in conjunction with choppers A and B, is designed to operate in two modes for these measurements. The following sections contain a discussion of how the detector is utilized for determination of particle flux, beam velocity, and its distribution.

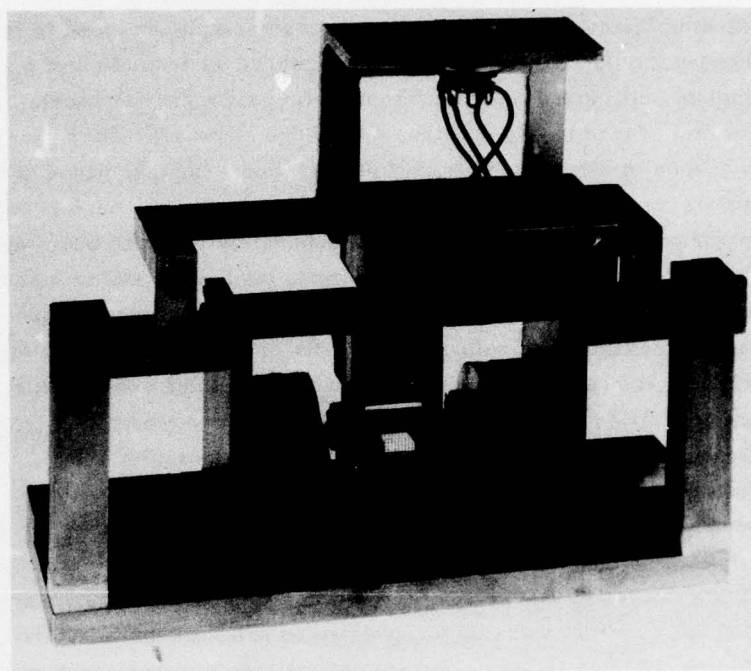12. Ramsey, N.F. (1956) Molecular Beams, Oxford University Press, London.

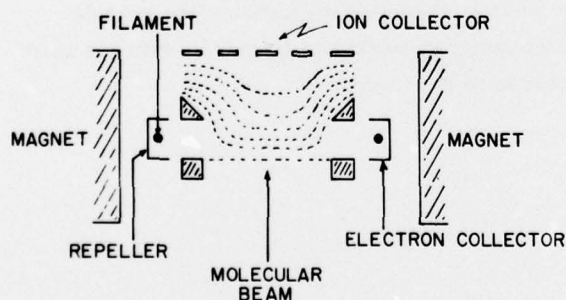Figure 6.   Photograph of the Molecular Beam Detector

Figure 7.   Representation of the Ionization Region of the Beam Detector

5.2.1 BEAM INTENSITY MEASUREMENTS

In this mode of operation, chopper A is moved into the path of the molecular beam. This chopper, we recall, has 8 equally spaced circular openings and has a 50 percent duty cycle. It chops the beam into segments that travel through the collision chamber and on into and through the detector. No target gases are introduced in the collision chamber so that the true unattenuated beam intensity is investigated. Background gases in the detector chamber give rise to background ions

17

which are discriminated against by the synchronous amplifier tuned to the beam chopping frequency. Ion currents are then measured as a function of p_o (pressure in the source) and converted to beam intensity (in particles/sec-ster).

Calibration of the detector requires knowledge of its efficiency in terms of the number of ions produced per beam particle. Since the magnitude of this ion current depends strongly upon the ionization cross section for each gaseous species, the detector efficiency has to be determined separately for each beam species employed. The best method of detector calibration, we found, was to measure the detector response (ions produced) for beams produced by an oven source whose intensity can be accurately calculated if oven pressure, temperature, aperture sizes, and geometry are known.[12] Such a source was constructed and mounted in the beam source chamber. The detector operating conditions were typically $I_{emission}$ = 10 mA, repeller potential = 50 V, and ion collection potential = 135 V. These values were chosen after extensive experimentation to optimize detector response and were used during calibration and actual intensity measurements for nozzle beams. For each beam species the magnitude of ion current against source pressure was obtained over pressure ranges appropriate to nozzle source operation. The resulting ion currents were then converted to beam intensities through the efficiency figure obtained in the calibration experiments.

Samples of intensity vs pressure for O_2 beams are shown in Figure 8 for three different nozzle-skimmer distances. In all cases, it is seen, intensity rises almost linearly with pressure until a plateau is reached. This maximum intensity occurs at higher pressures for longer nozzle-skimmer distance. Beyond this plateau, the background pressure in the chamber begins to interfere with the flow and causes a decrease in intensity because of scattering.
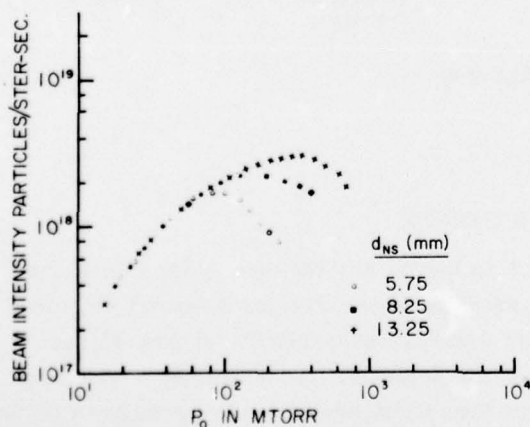

Figure 8. Intensity of an Oxygen Beam vs Nozzle Pressure for Three Nozzle-Skimmer Distances

Intensity curves for other species, and different gas mixture ratios have been obtained and recorded. Diagnostic measurements such as these were found a necessary part of the experimental program primarily for optimizing beam parameters for highest intensities.

5.2.2   BEAM VELOCITY MEASUREMENT

In the velocity measurement mode of the detector operation, Chopper B is moved into the path of the beam. This chopper, as has already been mentioned, has narrow radial slits and rotates at high speeds such that the beam open time is much smaller than the flight time of the particles to the detector. The detector then measures the arrival time of these beam particles. Because of a finite velocity distribution, the detector response is then a time of flight distribution which can be converted into velocity distribution. Figure 9 shows the schematics of the set-up used for the detector operating in the velocity mode. A photo cell is used to pick up a light signal at the instant the chopper is in the open position. This signal defines t = 0 for the beam particles in their flight to the detector and is also used to trigger the electronics. The ion signal from the ion collector is fed into a low noise amplifier and into a waveform eductor. The eductor, which basically is a synchronous amplifier, has 100 channels of variable width t. Each channel is super-imposed upon a portion of the repetitive wave form which is the time of flight distribution. The average value of the signal to each channel consists of the value of the wave form at that time and the random noise. Thus the eductor, which can integrate over a long period of time, measures the value of the repetitive signal since random noise averages to zero. The eductor (PAR TDH-9) consecutively samples the input signal over 100 channels each time it occurs and separately
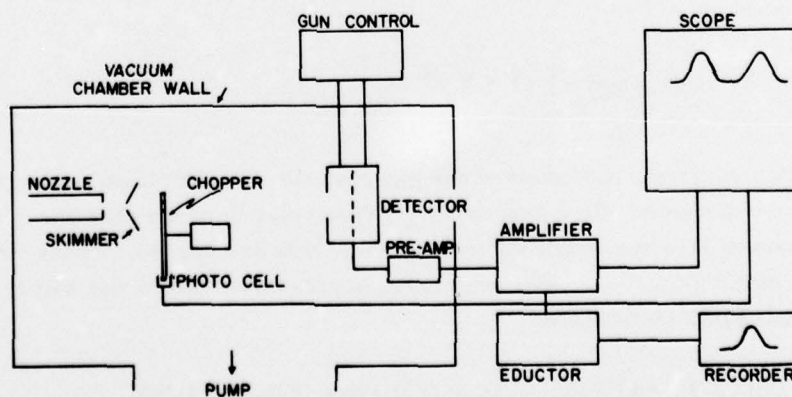

Figure 9. Schematic Representation of the Setup for Velocity Measurements

integrates the signal over each interval and stores it in a capacitor whose charge approaches the average value of the wave form during that interval. The contents of this "memory" are available at the output of the eductor and can be either displayed on a scope or recorded on a chart recorder through a slow readout terminal.

Figure 10 shows a time of flight distribution obtained for a beam of oxygen with a velocity of $\simeq$ 2 km/sec. The beam was obtained with 5 percent oxygen in 95 percent helium at room temperature. Due to the higher electron bombardment ionization cross section for O_2, as compared with that of He, the signal is almost entirely due to O_2.
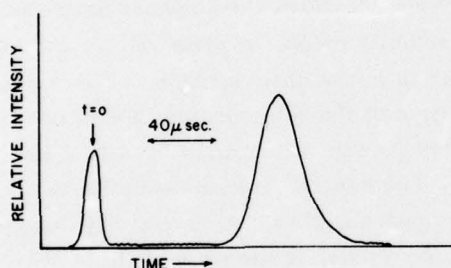

Figure 10. Sample Time-of-Flight Distribution Obtained for an Oxygen Beam

The time of flight distribution shown in Figure 10 represents instantaneous beam density at the detector as a function of travel time from chopper to detector. This signal can be used to obtain the velocity distribution function f(v) by different procedures.[13,14] The procedure most suitable to the present system is the one developed by Hagena and Henkes.[14] For particles on or near the beam axis, speed distribution is given by

$$f(v) = Av^3 \exp\left[\frac{-m}{2kT_e} \right] (V - V_o)^2$$

where A is a constant, m = mass of the gas particle, k = Boltzman constant. T_e = local flow temperature of the gas, and V_o = flow velocity of the stream. To completely characterize the distribution f(v), two values are needed. These are V_o and T_e. Expressions for these have been developed in reference 14 and will not be derived here. Final results are:

13. Anderson, J. B. and Fenn, J. B. (1965) Phys. Fluids, 8:780.
14. Hagena, O. F. and Henkes, W. (1960) Zeitschrift fur Naturforschun, 15a:851.

$$V_o = (L/t_m) \, h(a) \, ,$$

$$T_e = (mL^2/2k) \, t_m^{-2} \, g(a) \, ,$$

where

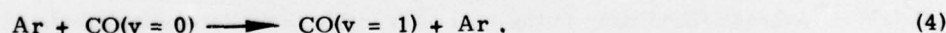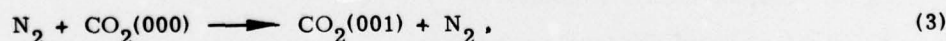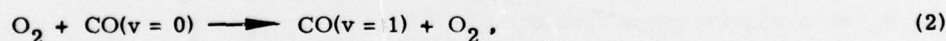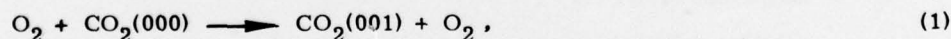$$h(a) = 1 - \frac{3}{2} g(a) \, , \quad a = t_m/t_1 \text{ or } t_m/t_2 \, ,$$

$$g(a) = \frac{(a-1)^2}{\ln_2 + 3(\ln a - a + 1)} \, .$$

In these equations L is the flight path, t_m is time at the maximum of the time of flight distribution measured, t_1 and t_2 are the times at half maximum in the distribution. It is seen that t_1, t_2, and t_m are the only experimentally measured times that are necessary to convert a TOF signal into velocity distribution.

Since the two half maximum signal times t_1 and t_2 are interchangeable in the above expressions, T_e and V_o could be determined two ways and thus a check of internal consistency of the method is available.

6. COLLISIONAL EXCITATION EXPERIMENTS

Among the reactions studied with the beam apparatus described in previous sections of this report are the following

$$O_2 + CO_2(000) \longrightarrow CO_2(001) + O_2 \, , \tag{1}$$

$$O_2 + CO(v = 0) \longrightarrow CO(v = 1) + O_2 \, , \tag{2}$$

$$N_2 + CO_2(000) \longrightarrow CO_2(001) + N_2 \, , \tag{3}$$

$$Ar + CO(v = 0) \longrightarrow CO(v = 1) + Ar \, . \tag{4}$$

The excited species $CO_2(001)$ and $CO(v = 1)$ would result in infrared radiation at 4.3 μm and 4.65 μm, respectively. The 4.3 μm band of CO_2 has an excitation energy $\simeq$ of 0.3 eV and the excitation energy for $CO(v = 1)$ is 0.26 eV. The beams of O_2, N_2, and Ar used in reactions (1) through (4) were fast beams produced by the heated seeded nozzle already described and their velocities were in the range of 3 km/sec to 4.5 km/sec. The relative energy of collisions in all four reactions listed were in the 2- to 3-eV range. This relative energy of collision is far in excess of the excitation energies of $CO_2(001)$ and $CO(v = 1)$, thus the reactions are

21

quite possible energetically. Beam intensities entering the collision chamber were 10^{16} to 10^{17} particles/sec, and target gas densities were 10^{13} cm^{-3}, corresponding to sub-mtorr pressures. For investigation of the 4.3 μm emission from CO_2 and the 4.65 μm band of CO, the infrared detectors were PbSe and InSb at liquid nitrogen temperature. These detectors were occasionally tested on an optical bench set-up equipped with a calibrated blackbody to ensure that they were functional under the conditions enumerated above. No emission from either CO_2 or CO were observed. Failure to observe any signal from the plume particles in these experiments can nevertheless be utilized to draw certain conclusions regarding the limitation of the apparatus and the magnitude of the cross sections under investigation. To arrive at these conclusions systematically, we first develop expressions for signal prediction and sources of noise. In terms of this signal to noise ratio, as will be seen, it is possible to put upper limit on cross sections and devise methods for increasing the S/N ratio such that measurement of cross sections could become possible.

Denoting the total number of excited target particles in the collision chamber by $N^{\ddagger}$ it can easily be shown that

$$N^{\ddagger} = (n_b n_t V_R \sigma_e)(D_S A_b) <t> , \qquad (5)$$

where

n_b = beam density in cm^{-3},

n_t = target density in cm^{-3},

V_R = relative collision velocity in cm/sec,

σ_e = excitation cross section cm^2,

D_S = collision chamber diameter,

A_b = beam cross sectional area (cm^2),

$<t>$ = average flight time to the wall of recoiled target particles (sec).

The first bracket in expression (5) is the production rate of excited target particles per unit volume and the second bracket is interaction volume and $<t>$, as mentioned, is time available for the excited particles to radiate before they reach the walls of the chamber where they are assumed to be completely deactivated. The relative collision velocity, V_R, is not simply the beam velocity distribution obtained from the time of flight measurement, since target particles in the chamber have their own velocity distribution which is not negligible. A method of arriving at the distribution in V_R and also a calculational technique for obtaining a value for $<t>$ will be developed in a separate AFGL report.

Equation (5) can be put in a different form that may be more useful. Noting that beam intensity (in particles/sec) is $n_b V_R A_B$, the equation becomes

$$N^\ddagger = (I_b n_t \sigma_e D_S) <t> , \tag{6}$$

where again the bracket is the production rate of excited target molecules per second and $<t>$ is defined above. In this form flux measurements can be directly inserted in (6) without a need to calculate beam densities n_b that appear in (5).

For the purposes of the present report, the final results of the extensive calculations to determine $<t>$ will be given here. To within a factor of 2, $<t>$ can be calculated from

$$<t> = \frac{D_s}{V_c} , \tag{7}$$

where V_c is the center of mass velocity of the colliding partners and is determined by the masses and laboratory velocities of the particles.

The infrared signal in terms of photons/sec incident on the infrared detector is

$$\text{signal(photons/sec)} = \mathcal{E} \frac{N^\ddagger}{\tau_{rad}} . \tag{8}$$

In this expression τ_{rad} is the radiative lifetime of the excited target particles and $\mathcal{E}$ is the efficiency of the integrating sphere measured to be 0.01. Inserting (6) in (8) the expression for the signal becomes

$$S = \mathcal{E} I_b n_t \sigma_e D_s \frac{<t>}{\tau_{rad}} . \tag{9}$$

The most severe source of noise in the present setup is the hot supersonic nozzle source which is operated in the 1000 K to 1500 K range to produce high beam velocities. Even though the beam is not mechanically chopped and is operated continuously, the inherent photon fluctuation from the dc operated hot background constitutes the largest component of noise. Other sources of background noise are the room temperature collision chamber and the infrared filter located directly at the detector. The noises due to the hot nozzle and chamber walls are that portion of their respective blackbody emission curves that go through the filter bandpass, whereas the filter noise itself is due to a portion of its blackbody curve up to detector cut-off wavelength. All these noises were calculated according to formulas available in the literature.[15] For a 1500 K nozzle source our calculations show

15. Wolfe, William L., Ed. (1965) Handbook of Military Infrared Technology, Office of Naval Research, Washington, D.C.

that total noise due to three sources enumerated above is 5×10^8 photons/sec. From (9) after insertion of the experimentally determined quantities I_b, n_t, $\mathcal{E}$, D_s and the calculated value of $\langle t \rangle$ from (7) the expression for signal to noise ratio then becomes

$$S/N = 10^{16} \frac{\sigma_e}{\tau_{rad}} , \qquad (10)$$

for a beam of O_2 incident on CO_2 at a relative velocity of 4.1 km/sec. Assuming that a S/N of 2 is tantamount to a measurement, and τ_{rad} for CO_2 of 2.5×10^{-3} second, σ_e has to be 5×10^{-19} cm^2. Since no signal was observed, this value can be interpreted as an upper limit on the excitation cross section. Similar reasoning has been applied at other velocities and with other collision partners. Table 1 is a summary of such analysis.

Table 1. Upper Limit on Excitation Cross Sections

Fast Beam	Target	V_r(km/sec)	τ_{rad}(msec)	σ_e Upper Limit (cm^2)
O_2	CO_2	4.1	2.5	5×10^{-19}
O_2	CO	4.4	31	3×10^{-18}
Ar	CO_2	3.9	2.5	10^{-20}

Cross sections of the magnitude shown in the last column of Table 1 are disappointingly low and point out the difficulty of conversion of kinetic energy to internal energy in heavy particle collisions, despite the fact that the relative kinetic energy available is several times larger than ΔE of the collisions under investigation. This low probability of excitation can qualitatively be explained by Massey's adiabatic hypothesis.[16] In a collision at relative velocity v, chances of a transition involving ΔE energy transfer will be small if

$$a \frac{\Delta E}{hv} >> 1 , \qquad (11)$$

where a is on the order of particle radii. Note that a/v is a collision time and $\Delta E/h$ is the period of the optically active electron. Stated differently, if collision takes place slowly, the system has time to adjust, thus transitions have a low

16. Massey, H.S.W. and Burhop, E.H.S. (1956) Electronic and Ionic Impact Phenomena, Oxford University Press, Oxford.

24

probability of occurring. For the collisions studied and listed in Table 1 it can be shown that (7) is satisfied. The adiabatic argument presented briefly here, unfortunately, does not provide the size of the cross section as a function of ΔE for fixed v, or as a function of v for fixed ΔE and a. The argument is presented only as an overall qualitative explanation for the smallness of cross sections we are attempting to measure. Implicit in the analysis of signal to noise ratios, given earlier in this section, is the suggestion for reducing the noise greatly by eliminating the background noise. It can be shown that if the collision chamber is cooled the background noise due to them can be almost entirely eliminated. Since the nozzle beam source has to be operated at elevated temperatures, provisions for baffling the radiation from it must be provided such that scattered radiation from the nozzle is reduced to absolute minimum. Guided by the results obtained in the experiments with the warm chamber and the analysis of S/N ratios, work is now in progress towards construction of a cold background collision chamber to replace the present room temperature collision chamber. In addition to appropriate band-pass filters, the infrared detector will be provided with circularly variable filters to obtain spectral band shapes of the emission from plume species that are vibrationally excited by fast beams of atmospheric species.

References

1. Kantrowitz, A. and Gray, J. (1951) Rev. Sci. Instr., 22:328.

2. Kistiakowsky, G. B. and Slichter, W. P. (1951) Rev. Sci. Instr., 22:333.

3. Becker, E. W. and Bier, K. (1954) Z. Naturforsch, 9a:975.

4. Anderson, J. B., Andres, R. P., and Fenn, J. B. (1966) Molecular Beams, J. Ross, Ed., Interscience, New York.

5. Sherman, F. S. (1963) Rarified Gas Dynamics, J. A. Laurman, Ed., Vol. II, Academic Press, New York.

6. Ashkenas, H. and Sherman, F. S. (1966) Rarified Gas Dynamics, J. H. deLeeuw, Ed., Academic Press, New York.

7. Klingelhofer, R. and Lohse, P. (1964) Phys. Fluids, 7:379.

8. Albright, R. G., Peeters, J. Bourguignon, M., LeRoy, R. L., and Deckers, J. M. (1966) Rarefied Gas Dynamics, J. H. DeLeeuw, Ed., Academic Press, New York.

9. French, J. B. and O'Keefe, D. R. (1966) Rarefied Gas Dynamics, J. H. deLeeuw, Ed., Academic Press, New York.

10. Dolan, C. P. (1971) Rev. Sci. Instr., 42:1228.

11. Taylor, J. B. (1930) Phys. Rev., 35:375.

12. Ramsey, N. F. (1956) Molecular Beams, Oxford University Press, London.

13. Anderson, J. B. and Fenn, J. B. (1965) Phys. Fluids, 8:780.

14. Hagena, O. F. and Henkes, W. (1960) Zeitschrift fur Naturforschun, 15a:851.

15. Wolfe, William L., Ed. (1965) Handbook of Military Infrared Technology, Office of Naval Research, Washington, D. C.

16. Massey, H. S. W. and Burhop, E. H. S. (1956) Electronic and Ionic Impact Phenomena, Oxford University Press, Oxford.